Available online at www.sciencedirect.com
ScienceDirect
Trans. Nonferrous Met. Soc. China 27(2017) 1716−1724
Transactions of Nonferrous Metals Society of China
www.tnmsc.cn

Fabrication of carbon nanotube reinforced AZ91D composite with superior mechanical properties

Qiu-hong YUAN[1,2], Dong-ming FU[1], Xiao-shu ZENG[1], Yong LIU[1]

1. Department of Materials Engineering, Nanchang University, Nanchang 330031, China;
2. Xinyu Institute of New Energy, Xinyu University, Xinyu 338000, China

Received 8 November 2015; accepted 14 June 2016

Abstract: AZ91D alloy composites with 1.0% CNTs have been fabricated by a method combined ball milling with stirring casting. The composite was investigated using optical microscopy(OM), X-ray diffraction(XRD), Fourier transform infrared spectroscope (FT-IR), scanning electron microscope (SEM), transmission electron microscope (TEM) and room temperature (RT) tensile test. The results show that CNTs were homogeneously distributed in the matrix and maintained integrated structure. The yield strength and ductility of AZ91D/CNTs composite were improved by 47.2% and 112.2%, respectively, when compared with the AZ91 alloy. The uniform distribution of CNTs and the strong interfacial bonds between CNT and the matrix are dominated to the simultaneous improvement of yield strength and ductility of the composite. In addition, the grain refinement as well as the finer β phase ($Mg_{17}Al_{12}$) with homogenous distribution in the matrix can also slightly assist to the enhancement of the mechanical properties of the composite.

Key words: magnesium alloy; carbon nanotube; composite; casting; mechanical properties

1 Introduction

Metal matrix composites (MMCs) are gaining popularity due to their improved mechanical properties over the monolithic metals [1,2]. Among the MMCs, magnesium (Mg) matrix composites are attracting increasing attention as lightweight structural materials because they have low density, high strength, superior creep resistance and high damping capacity, which can be widely used in aerospace, electronics and automotive industries [3,4]. Carbon nanotubes (CNTs) is the excellent reinforcement of Mg-based composite due to its fantastic mechanical and physical properties, such as high elastic modulus (~1 TPa), excellent tensile strength (~150 GPa) and low density (1.8 g/cm^3) [5,6]. CNTs are being employed as the reinforcement in the matrix of Mg alloy. At present, the challenges in the synthesis of CNTs reinforced Mg-based composite are shown as follows [7−9]: 1) a uniform dispersion of CNTs in the matrix of Mg alloy; 2) tailor a stronger interfacial bonds between CNTs and Mg alloy; 3) how to avoid the losses of CNTs during processing, and 4) a fabrication technique suitable for a large scale of production. To solve the above problems, some attempts have been conducted on magnesium matrix composites containing CNTs. For example, AZ91D alloy composite with CNTs has been synthesized by power metallurgy (PM) with following extruding process [10]. The results show that the ultimate tensile strength of the composite was enhanced from 315 MPa to 388 MPa. However, the ductility of the composite was greatly reduced from 14% to 5%. LIU et al [4] fabricated AZ91D alloy composite with 1.5% CNTs by mechanical stirring and high-intensity ultrasonic dispersion process and achieved simultaneously improvement in tensile strength and ductility. A method combined ball-milling with ultrasonic melt processing was developed to fabricate CNTs reinforced Mg−6.0Zn composite and obtain the significant improvement in tensile strength as well as ductility [11]. PM is the effective processing to uniform disperse CNTs in the matrix of metals. However, the processing cycle of PM is longer and costly and only suitable for the fabrication of parts with small

Foundation item: Project (51464034) supported by the National Natural Science Foundation of China; Projects (GJJ151309, GJJ151010) supported by the Education Department of Jiangxi Province, China
Corresponding author: Yong LIU; Tel/Fax: +86-791-83968992, E-mail: liuyong@ncu.edu.cn
DOI: 10.1016/S1003-6326(17)60194-8

dimensions. The ultrasonic melt processing can not only disperse CNTs uniformly, but also significantly improve the wettability between CNTs and the matrix of Mg alloy. However, such processing is only effective to treat small dimension samples. It is very inefficient to fabricate parts with larger dimensions. Thus, it is very necessary to develop a novel method for the synthesis of Mg-CNT composite parts with large dimension and superior performance.

It has been reported that CNTs have a good compatibility with the Mg melt [11]. Given this, the casting processing may be a promising technology to fabricate Mg-CNT composite. However, it is very difficult to disperse CNTs directly in the Mg melt because they are easily entangled due to the strong Van der Waal's force. Therefore, a pre-dispersion of CNTs is necessary before adding CNTs to the Mg melt. In general, the ball-milling and the surface modification of CNTs are the primary approaches used in the pre-dispersion of CNTs. The surface modification of CNTs is effective in dispersing CNTs in the matrix, but it is too complicated and inefficient in production. In comparison, ball-milling is a sample and effective processing in production [12,13]. Moreover, the ball-milling processing can be easily optimized by adjusting the milling time, rotational speed, and ball-to-powder mass ratio. Therefore, the mechanical ball milling is a promising candidate for CNTs pre-dispersion. After the pre-dispersed CNTs were added to the Mg melt, the mechanical stirring may effectively disperse pre-dispersed CNTs in the matrix of Mg alloy. However, the related researches on CNTs reinforced Mg matrix composites are rarely reported.

In this study, an optimized method combined ball milling with stirring casting was used to prepare CNTs reinforced AZ91D alloy composite. The microstructure and mechanical properties of AZ91D composite containing 1.0% CNTs were studied in detail.

2 Experimental

The commercial AZ91D alloy with the composition of 9.0% Al, 1.0% Zn, and 0.4% Mn was used as the raw material [14]. Metal powders (pure Mg, Al, and Zn powders with about 75 μm in diameter) and multi-wall carbon nanotubes [15] (>90% purity, 5−30 nm in diameter and 1−10 μm in length) were used for the preparation of CNTs block.

AZ91D composite reinforced with 1.0% CNTs was fabricated by an optimized method combing ball milling with stirring casting. Firstly, CNTs were previously dispersed in AZ91 alloy powder by ball milling, the details of which are shown in the previous study [8]. The mixed powders were then compacted in a 40 mm-wide and 200 mm-high cylinder mold under a hydraulic pressure of 100 kN to prepare a CNTs block. Secondly, AZ91D alloy was melted at 993 K under a protective atmosphere of CO_2 and SF_6 to avoid burning. The preheated CNTs block (393K) was then added into the alloy melt and heated to 1073 K. After the CNTs block was melted completely, the mixture was cooled to 993 K and stirred for 3 min with a rate of 100 r/min using a mild steel impeller. The mixture melt was then poured into a permanent mold preheated to 473 K to prepare a composite sample. For comparison, the sample of AZ91D alloy without CNTs was also prepared by the same process without mechanical stirring.

The uniaxial tensile tests were performed with an initial strain rate of 0.001 s^{-1} at room temperature (UTM5105). Optical microscope (OM, OLYMPUS BX-51), X-ray diffraction (XRD, Shimadzu LAB-X XRD-6000), Fourier transform infrared spectroscope (FT-IR, TENSOR 27 FTIR spectrometer), scanning electron microscope (SEM, FEI Quanta200F), and transmission electron microscope (TEM, FEI TECNAI G2 S-TWIN F20) were used to characterize the microstructure, CNTs distribution and phase component of samples. The volume fraction of second phase in the composite was determined by an image analyzer on metallographic sections. The solution heat treatment (T4) with the holding time of 18 h at 686 K and followed quenching in air was applied on the samples of the composite for the accurate assessment of the grain refinement by CNTs. The FT-IR powder sample was prepared by crushing a small piece of AZ91/CNTs composite.

3 Results and discussion

3.1 Distribution of CNTs in CNTs block

In order to check out the distribution of CNTs in the block, the fracture surface of CNTs block (Fig. 1(b)) was provided instead of optical microstructure, since CNTs were hardly observed by using optical microscopy. Morphologies of milled mixture powders with ball-milling (Fig. 1(a)) was also given for comparison. It can clearly be seen that CNTs are uniformly embedded in the crushed metal powders after ball-milling, as shown in Fig. 1(a). Furthermore, as also can be seen in Fig. 1(b) that there are some individual CNTs were embedded in the CNTs block and the clusters of CNTs have not been observed on the fractured surface. Those observations above indicate that CNTs have been uniformly dispersed in the CNTs block with such ball-milling process. In general, metal powders will be crushed into small particles or flaky morphology due to the shear force during ball milling. On the other hand, CNTs were shortened and CNTs clusters were broken down by

shearing force [12]. Then, CNTs were gradually embedded inside the metal powders through plastic deformation of those metal powders under the impact of the balls during the ball milling.

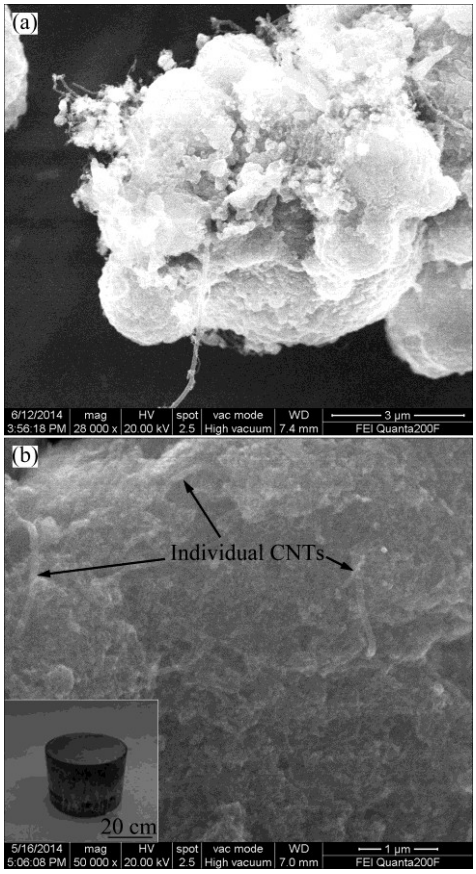

Fig. 1 SEM images of mixture powders with ball-milling (a) and fracture surface of CNTs block (b) (The inset in (b) shows the photograph of a CNT block sample)

3.2 Microstructure characterization

Figure 2 shows the XRD patterns of AZ91D alloy and AZ91D/CNTs composite. Both the samples are composed of primary α-Mg and β phase ($Mg_{17}Al_{12}$). In addition, no peaks of carbon were found in the XRD patterns of AZ91D/CNTs composite. It could be attributed to the low content of CNTs in the matrix [16], in agreement with the previous study [17]. Furthermore, it can be noted that the intensity of β phase in AZ91D/CNTs composite is stronger than that of AZ91D alloy, which suggests that the AZ91D/CNTs composite contains more volume fraction of β phase, in agreement with the previous study [8]. It has been reported that CNTs can enhance the heat dissipation capacity of the Mg liquid and result in increasing the cooling rate of the Mg melt [18], which is beneficial to the precipitation of β phase in the matrix. Therefore, more volume fraction of β phase precipitated in AZ91/CNTs composite can be attributed to the improved cooling rate of the Mg melt by CNTs due to its excellent thermal conductivity.

Figure 3 shows the microstructure of AZ91D alloy and AZ91D/CNTs composite with/without solution treatment. As shown in Fig. 3(a), the as-cast AZ91D alloy mainly consists of massive net-like β phase along the grain boundary and the lamellar β phase within the grain or near to the massive β phase. However, as shown in Fig. 3(b), the β phase exhibits more finer and homogenous in the AZ91D/CNTs composite, as compared to the AZ91D alloy. Furthermore, the total volume fraction of β phase was increased from 13.2% in AZ91D alloy to 14.7% in AZ91D/CNTs composite, in agreement with the XRD results above. The homogenous distribution of β phase in AZ91D/CNTs composite may be attributed to the mechanical stirring, since a strong stirring always leads to the uniform distribution of solute elements, and results in the homogenous distribution of β phase in the matrix [19]. Therefore, the ball milling and stirring casting used in this study is beneficial to the uniform distribution of CNTs and β phase in the matrix.

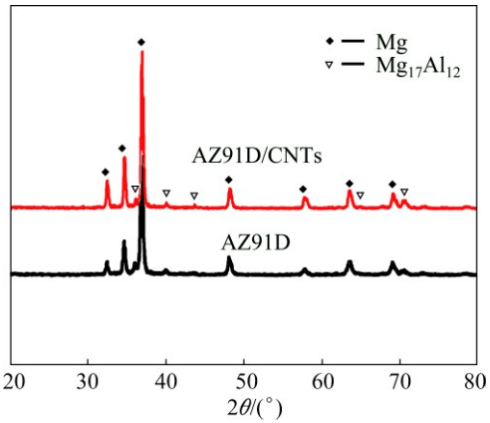

Fig. 2 XRD patterns of AZ91D alloy and AZ91D/CNTs composite

In order to more clearly identify the grain size of the as-cast AZ91 alloy and AZ91D/CNTs composite, the solution heat treatment was conducted on the corresponding samples. As shown in Figs. 3 (c) and (d), the average grain size of α-Mg is refined from (136.8±5) μm (AZ91D alloy) to (65.3±3.5) μm (AZ91D/CNTs composite).

One criterion of heterogeneous nucleation is that the Bramfitt planar disregistry of nucleation planes between new phase and mother phase is less than 15% [20]. The CNT has hexagonal structure with the lattice constants of a=2.47Å, c=6.724Å. The Mg has hexagonal structure with lattice constants of a=3.18 Å and c=5.19Å [21]. Therefore, the Bramfitt planar disregistry δ between the low index planes can be calculated using the following formula [20]:

$$\delta_{(h\,k\,l)_n}^{(h\,k\,l)_s}=\sum_{i=1}^{3}\{|\,d[u\,v\,w]_s^i\cos\theta-d[u\,v\,w]_n^i\,|/d[u\,v\,w]_n^i\}/3\times100\%$$

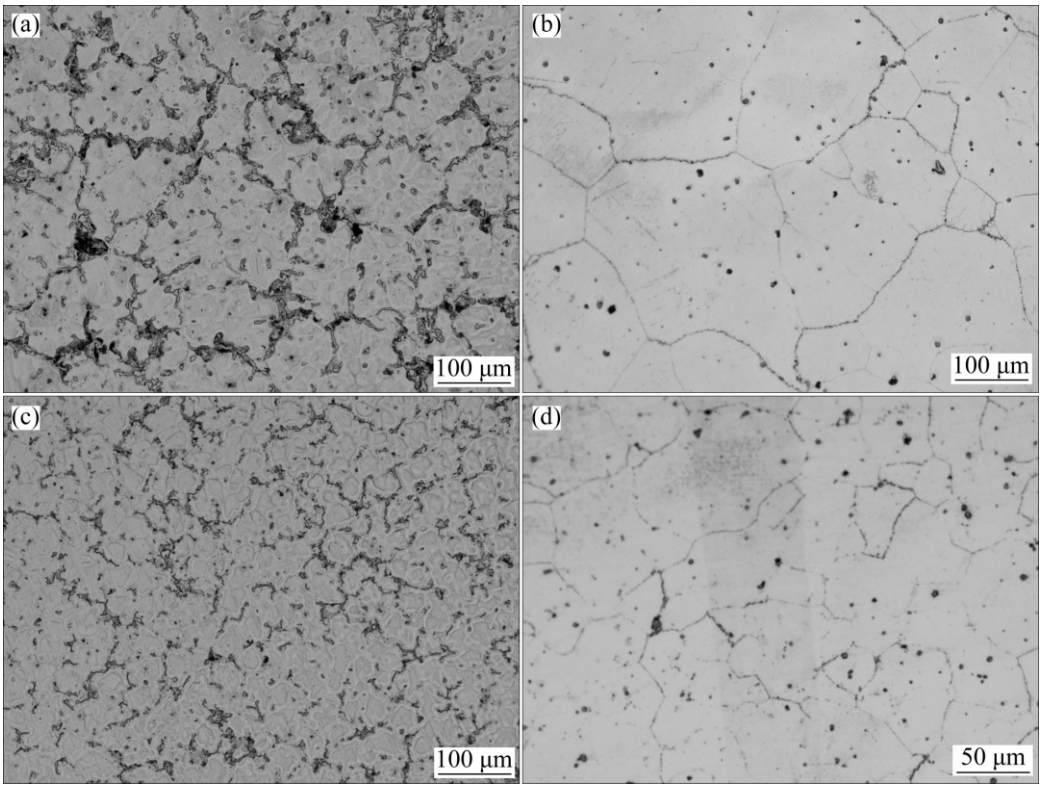

Fig. 3 Microstructure of AZ91D alloy without (a−b) and with (c−d) solution treatment (The average grain size values are labeled in (c) and (d))

where $(h\ k\ l)_s$ and $(h\ k\ l)_n$ are the low index planes of the substrate and nucleus, respectively, $[u\ v\ w]_s$ is the low index direction in $(h\ k\ l)_s$, $(h\ k\ l)_n$ is the low index plane in the nucleated solid, $[u\ v\ w]_n$ is the low index direction in $(h\ k\ l)_n$, $d[u\ v\ w]_s$ is the interatomic spacing along the $[u\ v\ w]_s$, $d[u\ v\ w]_n$ is the interatomic spacing along the $[u\ v\ w]_n$, and θ is the angle between the $[u\ v\ w]_s$ and $[u\ v\ w]_n$.

The Bramfitt planar disregistries δ between CNT and α-Mg along possible crystallographic orientation relationships (ORs) are listed in Table 1. It can clearly be seen that the OR of $(0001)_{Mg}//(0001)_{CNT}$ exhibits the smallest disregistry value of 29.96%, which is greatly larger than 15%. This suggests that CNT cannot act as the heterogeneous nuclei for the grain refinement of AZ91D alloy theoretically. LU et al [22] reported that adding Al_4C_3 to Mg−Al alloys could effectively result in a grain-refining of the matrix. Because the Bramfitt planar disregistry between Al_4C_3 (a=3.3388 Å, c=24.996 Å) and the matrix is calculated as 4.05%, which is less than 15%. Therefore, Al_4C_3 particles can serve as the heterogeneous nucleation sites and result in a change of the microstructure. It has been verified by CI et al [23] that a reaction between CNTs and Al to form the Al_4C_3 compound can occur at the temperature above 823 K. Therefore, the formation of Al_4C_3 may be one of the main reasons in the grain refinement by CNTs because there exists Al element in AZ91D alloy and the process temperature here is 1073 K which is much higher than 823 K. The Al_4C_3 compound has not been detected by XRD in this AZ91D/CNTs composite, which may be attributed to the low content of Al_4C_3 in the composite. In order to further confirm this point, the interfacial reaction between CNTs and AZ91 alloy will be highlighted in our future work.

In addition, it was confirmed that incorporation of a small amount of CNTs in Mg−2.0Zn alloy, the secondary dendrite arm spacing of Mg−2.0Zn alloy was refined significantly due to the improved thermal conductivity of the molten metal by CNTs [18]. CNTs have an excellent thermal conductivity greater than 2500 W/(m·K). They will increase the heat transfer ability of liquid, which has been confirmed by many studies on nanoflows [24,25]. Therefore, a homogenous dispersion of CNTs in the Mg liquid will enhance the heat dissipation capacity of the liquid alloy, which is crucial to increase the cooling rate in the area around CNTs. The improved cooling rate will result in a finer grain size of the Mg matrix. In addition, a homogenous dispersion of CNTs in the Mg liquid could effectively serve as obstacles to the growth of grains of α-Mg when solidification occurs. Therefore, the microstructure refinement of Mg alloys can be ascribed to the homogenous dispersion of CNTs in the matrix and the improved cooling rate of liquid Mg alloy by CNTs.

Table 1 Bramfitt planar disregistry δ between CNT and α-Mg along possible ORs

Match planes	$[u\ v\ w]_{CNT}$	$[u\ v\ t\ w]_{Mg}$	θ/(°)	$d[u\ v\ w]_{CNT}$/nm	$d[u\ v\ t\ w]_{Mg}$/nm	δ/%
$(0001)_{CNT}$// $(0001)_{Mg}$	[100]	$[10\bar{1}0]$	0	0.247	0.321	29.96
	[110]	$[11\bar{2}0]$	0	0.247	0.321	
	[010]	$[01\bar{1}0]$	0	0.247	0.321	
$(0001)_{CNT}$// $(10\bar{1}1)_{Mg}$	$[\bar{2}\bar{1}0]$	[0001]	0	0.428	0.521	66.45
	[010]	$[01\bar{1}0]$	0	0.247	0.321	
	$[\bar{1}00]$	$[01\bar{1}1]$	1.65	0.247	0.612	

3.3 FT-IR spectra analysis

Figure 4 shows the FT-IR spectra of as-received pure CNTs and AZ91D/CNTs composite powders. It can clearly be seen that the broad bands at 3430 cm^{-1} and 1643 cm^{-1} are attributed to the hydroxyl (—OH) stretching, which resulted from the absorption of moisture in the air. The bands at 860, 1064, 1463 and 1725 cm^{-1} are assigned to aromatic C—H out-of-plane, C—O/C—O—C vibrations of phenol/carboxyl groups, CH_2/CH_3 banding vibrations and C═O vibrations of carboxyl, respectively [26,27]. All of these FR-IR absorption bands can be associated with CH_2 or CH_3 stretching vibrations. Moreover, it can also be seen in Fig. 4 that the peaks of AZ91D/CNTs composite powders are matched very well with those of CNTs. This suggests that not only the existence of CNTs in the composite, but also the structure of CNTs in the matrix was not destroyed after the ball milling and the following casting process.

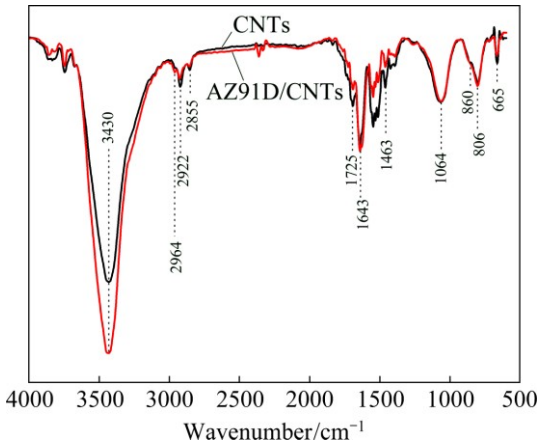

Fig. 4 FT-IR spectra of as-received CNTs and AZ91D/CNTs composite

3.4 Mechanical properties

Typical stress−strain curves of AZ91D alloy and AZ91D/CNTs composite are shown in Fig. 5. Table 2 presents the mechanical properties of AZ91D alloy and its composite, including the corresponding parameters of some particle-reinforced AZ91D composites for comparison. As shown in Fig. 5 and Table 2, the yield strength (YS), ultimate tensile strength (UTS) and elongation of AZ91D alloy with 1.0% CNTs reached 113.5 MPa, 254 MPa and 15.7%, increasing by 47.2%, 63.9% and 112.2%, respectively, as compared to that of AZ91 alloy. In addition, as shown in Table 2, only the AZ91D/CNTs composite exhibits the simultaneous improvement in tensile strength and ductility, as compared to the particle-reinforced AZ91D composites [4,28−30]. This also proves the superiority of CNTs in enhancing the performance of Mg alloy.

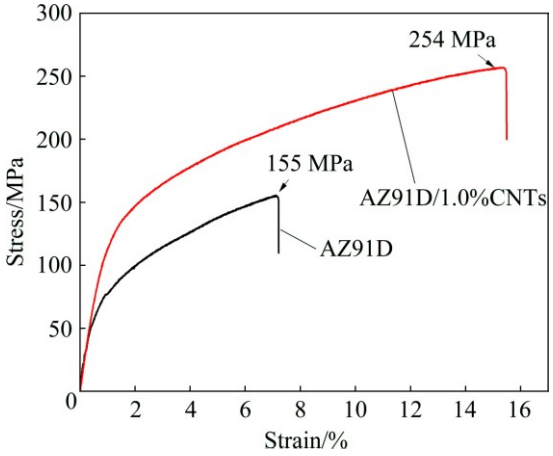

Fig. 5 Typical stress−strain curves of AZ91D alloy and AZ91D/CNTs composite

Table 2 Mechanical properties of as-cast AZ91D alloy and AZ91D/CNTs composite

Material	Grain size/μm	UTS/ MPa	YS/ MPa	Ductility/ %	WOF/ $(MJ\cdot m^{-3})$	Ref.
AZ91D	138.6±5.0	155	77.1	7.4	8.28	This work
AZ91D/ CNTs	65.3±3.5	254	113.5	15.7	31.21	This work
AZ91D/ 1.0%AlN	–	185	144	3.0	–	[28]
AZ91D/ 1.5%CNTs	–	157	104	1.28	–	[4]
AZ91/ 10%TiC	–	214	–	4.0	–	[29]
AZ91D/ 2.0%Y	–	145.9	81.9	3.2	–	[30]

Figure 6 shows the TEM images of AZ91D/CNTs composite near the fracture surface area of the tensile sample. It can be seen that a larger number of dislocations were tangled around the CNT, as shown in Fig. 6(a). This suggests that CNT could act as obstacles and provide an effective way to restrain the dislocation motion. This will lead to the generation of back stress, which could prevent the further movement of dislocation and result in the increment of yield stress. In addition, as shown in Fig. 6(b), some individual CNTs can clearly be observed and no obvious microstructure damage was found on the carbon nanotubes. All these suggest that CNTs are distributed homogeneously and its well-integrated structure was retained in the composite. Moreover, there is no nanopores were detected at the CNTs/matrix interface in the matrix, as shown in Fig. 6(b). This indicates that strong interfacial bonding between CNT and the matrix was formed in the composite. This ensures that the load can be effectively transferred from the matrix to CNTs when loading. As a result, a full reinforcing effect by CNTs has occurred. In addition, CNTs can activate the non-basal plane slip of Mg alloy [31,32], which is beneficial to the deformation of Mg alloy, and thus results in an improvement in ductility.

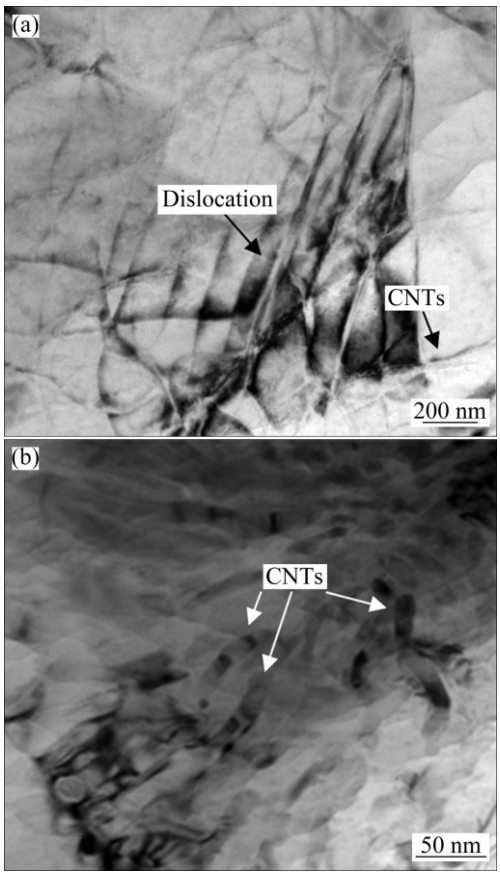

Fig. 6 TEM images of AZ91D/CNTs composite after tensile near fracture surface: (a) Dislocation around CNTs; (b) CNTs distribution in matrix (marked with arrows)

On the other hand, the finer grains will lead to a higher YS according to the Hall−Petch relationship. It has been reported that both the yield strength and ductility of the composite can be improved by grain refinement [33,34]. Additionally, the mechanical properties of Mg−Al alloy are also influenced by both the distribution and morphology of β phase [35]. A fine distribution of the β phase helps to withstand a large deformation before fracture [36]. Generally, the discontinuous β phase with a homogenous distribution play an important role in both the strength and ductility of the matrix due to the movement of dislocation and delay in the failure of material during deformation by those β phases.

Based on the analysis above, it can be concluded that the uniform distribution of CNTs and the strong interfacial bonds between CNTs and the matrix of Mg alloy are dominated to the simultaneous improvement of tensile strength and ductility of the composite. In addition, the grain refinement as well as the finer β phase with homogenous distribution in the matrix can also slightly assist to the enhancement of the mechanical properties of the composite.

The work of fracture (WOF) is considered as the ability of the material to absorb energy up to fracture under tensile loading, which can be calculated by the area under the engineering stress−strain curve up to the point of fracture [37]. The WOF of AZ91D/CNTs composite is improved by 276.9%, as compared to AZ91D alloy, as shown in Table 2. This reveals that the damage tolerant capability of AZ91D alloy can be significantly improved by CNTs.

3.5 Fracture mechanism

Figure 7 shows the SEM images of the fracture surfaces of AZ91D alloy and AZ91D/CNTs composite. Both types of the materials samples exhibit dimple-like structure, which reveals ductile fracture behavior, as shown in Figs. 7(a) and (b). Moreover, the fracture surface of AZ91D/CNTs composite exhibits much more and homogenous dimples than that of AZ91D alloy, indicating a superior ductility, as compare to AZ91D alloy. It has been reported that addition of CNTs into the matrix of Mg alloy could increase the ductility of the Mg-based composite because more slip systems have been activated by CNTs [31]. In addition, some ruptured CNTs individually exposed outside the fracture surface were clearly observed in Fig. 7(c) (marked with white arrows), indicating that the load transfer was operative. Furthermore, as shown in Fig. 7(d), it can clearly be seen that CNTs with net structure were embedded in the matrix, indicating a homogeneous distribution. Those results are consistent with those of mechanical properties test for the AZ91D/CNTs composite. This also confirmed

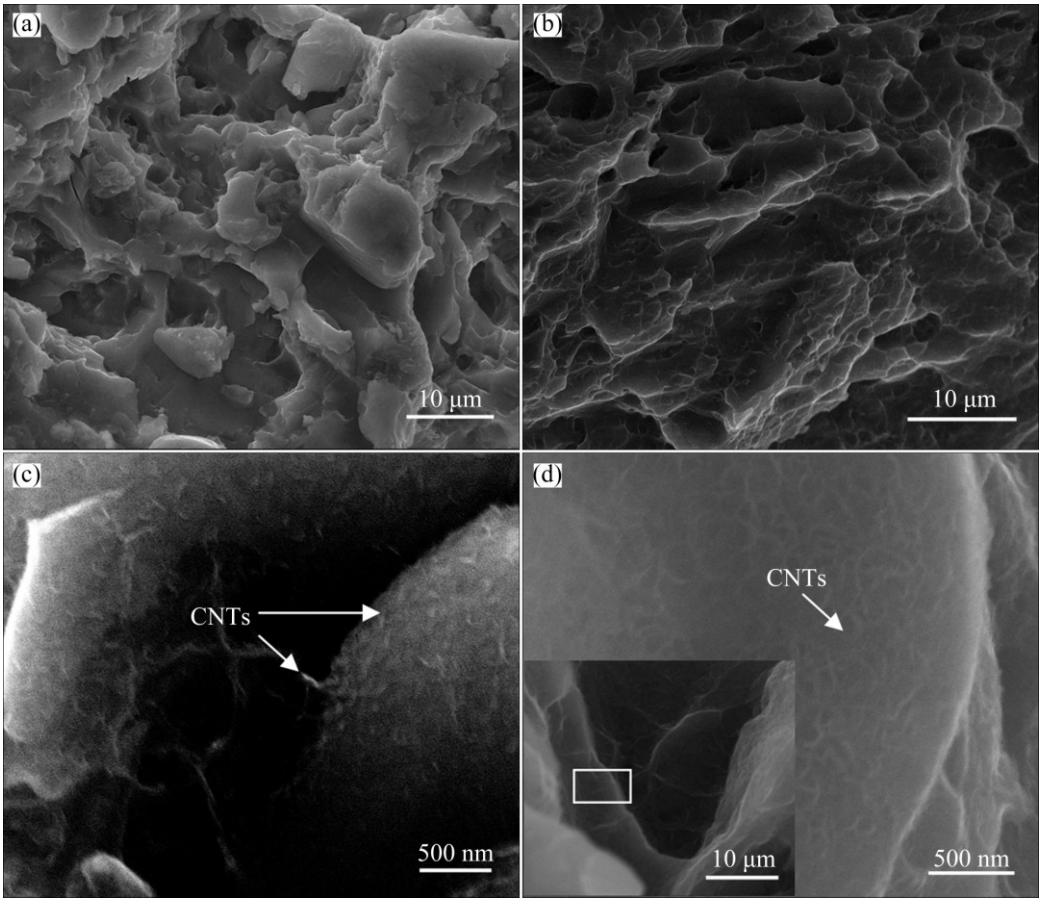

Fig. 7 SEM images of fracture surface of AZ91D alloy (a) and AZ91D/CNTs composite (b−d) ((d) is high magnification image of corresponding region marked by white rectangle in inset)

that the method combined ball milling with stirring casting is appropriate to fabricate AZ91D/CNTs composite parts with large dimension and superior performance.

4 Conclusions

1) CNTs can be homogeneously distributed in the matrix by using an optimized method combined ball milling with stirring casting. The uniform distributed CNTs can effectively refine the grains of α-Mg and β phase and improve their homogeneous distribution in the matrix.

2) The YS, UTS, elongation, and WOF of AZ91D/CNTs composite were increased by 47.2%, 63.9%, 112.2%, and 276.9%, respectively, as compared to AZ91D alloy. The uniform distribution of CNTs and the strong interfacial bonds between CNT and the matrix of Mg alloy are dominated to the simultaneous improvement of tensile strength and ductility of the composite. In addition, the grain refinement as well as the finer β phase with homogenous distribution in the matrix can also slightly assist to the enhancement of the mechanical properties of the composite.

3) The findings in this study suggest that the ball milling combined with stirring casting is appropriate to fabricate AZ91D/CNTs composite parts with large dimension and superior performance.

References

[1] ZHANG Yang, WU Guo-hua, LIU Wen-cai, ZHANG Liang, SONG Pang, DING Wen-jiang. Effects of processing parameters on microstructure of semi-solid slurry of AZ91D magnesium alloy prepared by gas bubbling [J]. Transactions of Nonferrous Metals Society of China, 2015, 25(7): 2181−2187.

[2] YANG Ling, HOU Hua, ZHAO Yu-hong, YANG Xiao-min. Effect of applied pressure on microstructure and mechanical properties of Mg−Zn−Y quasicrystal-reinforced AZ91D magnesium matrix composites prepared by squeeze casting [J]. Transactions of Nonferrous Metals Society of China, 2015, 25(12): 3936−3943.

[3] NAI M H, WEI J, GUPTA M. Interface tailoring to enhance mechanical properties of carbon nanotube reinforced magnesium composites [J]. Materials & Design, 2014, 60(8): 490−495.

[4] LIU Shi-ying, GAO Fei-peng, ZHANG Qiong-yuan, ZHU Xue, LI Wen-zhen. Fabrication of carbon nanotubes reinforced AZ91D composites by ultrasonic processing [J]. Transactions of Nonferrous Metals Society of China, 2010, 20(7): 1222−1227.

[5] LI C D, WANG X J, LIU W Q, WU K, SHI H L, DING C, HU X S, ZHANG M Y. Microstructure and strengthening mechanism of carbon nanotubes reinforced magnesium matrix composite [J]. Materials Science and Engineering A, 2014, 597(4): 264−269.

[6] XU Qiang, ZENG Xiao-shu, ZHOU Guo-hua. Mechanical properties of CNTs/AZ31 composites prepared by adding CNTs block with plunger [J]. The Chinese Journal of Nonferrous Metals, 2010, 2(20): 189−194. (in Chinese)

[7] BHAT A, BALLA VK, BYSAKH S, BASU D, BOSE S, BANDYOPADHYAY A. Carbon nanotube reinforced Cu−10Sn alloy composites: Mechanical and thermal properties [J]. Materials Science and Engineering A, 2011, 528(22−23): 6727−6732.

[8] ZENG Xiao-shu, ZHOU Guo-hua, XU Qiang, XIONG Y, LUO C, WU J. A new technique for dispersion of carbon nanotube in a metal melt [J]. Materials Science and Engineering A, 2010, 527(20): 5335−5340.

[9] LI Hai-peng, FAN Jia-wei, KANG Jian-li, ZHAO Nai-qin, WANG Xue-xia, LI Bao-e. In-situ homogeneous synthesis of carbon nanotubes on aluminum matrix and properties of their composites [J]. Transactions of Nonferrous Metals Society of China, 2014, 24(7): 2331−2336.

[10] SHIMIZU Y, MIKI S, SOGA T, ITOH I, TODOROKI H, HOSONO T, SAKAKI K, HAYASHI T, KEM YA, ENDO M, MORIMOTO A, KOIDE A. Multi-walled carbon nanotube-reinforced magnesium alloy composites [J]. Scripta Materialia, 2008, 58(4): 267−270.

[11] SHI Hai-long, WANG Xiao-jun, LI Cheng-dong, HU Xiao-shi, DING Chao, WU Kun, HUANG Yu-dong. A novel method to fabricate CNT/Mg-6Zn composites with high strengthening efficiency [J]. Acta Metallurgica Sinica (English Letters), 2014, 27(5): 909−917.

[12] LIU Z, XU S, XIAO B, XUE P, WANG W, MA Z. Effect of ball-milling time on mechanical properties of carbon nanotubes reinforced aluminum matrix composites [J]. Composites Part A: Applied Science and Manufacturing, 2012, 43(12): 2161−2168.

[13] HAO Xiao-ning, ZHANG Hai-ping, ZHENG Rui-xiao, ZHANG Yi-tan, AMEYAMA K, MA Chao-li. Effect of mechanical alloying time and rotation speed on evolution of CNTs/Al-2024 composite powders [J]. Transactions of Nonferrous Metals Society of China, 2014, 24(7): 2380−2386.

[14] POLMEAR I. Magnesium alloys and applications [J]. Materials Science and Technology, 1994, 10(1): 1−16.

[15] YUAN Qiu-hong, ZENG Xiao-shu, LIU Yong, LUO Lei, WU Jun-bin, WANG Yan-chun, ZHOU Guo-hua. Microstructure and mechanical properties of AZ91 alloy reinforced by carbon nanotubes coated with MgO [J]. Carbon, 2016, 96(1): 843−855.

[16] CULLITY B, STOCK S. Elements of X-ray diffraction [M]. 3rd ed. London: Prentice-Hall, 2001.

[17] PARAMSOTHY M, CHAN J, KWOK R, GUPTA M. Addition of CNTs to enhance tensile /compressive response of magnesium alloy ZK60A [J]. Composites Part A: Applied Science and Manufacturing, 2011, 42(2): 180−188.

[18] ZENG Xiao-shu, LIU Yong, HUANG Qiu-yu, ZENG Gang, ZHOU Guo-hua. Effects of carbon nanotubes on the microstructure and mechanical properties of the wrought Mg−2.0Zn alloy [J]. Materials Science and Engineering A, 2013, 571(6): 150−154.

[19] KIM Y M, YIM C D, YOU B S. Grain refining mechanism in Mg−Al base alloys with carbon addition [J]. Scripta Materialia, 2007, 57(8): 691−694.

[20] BRAMFITT B. Planar lattice disregistry theory and its application on heterogistry nuclei of metal [J]. Metallurgical Transactions A, 1970, 1: 1987−95.

[21] AVEDESIAN M M. Magnesium and magnesium alloys [M]. USA: ASM International, 1999: 7−10.

[22] LU L, DAHLE A, STJOHN D. Grain refinement efficiency and mechanism of aluminium carbide in Mg−Al alloys [J]. Scripta Materialia, 2005, 53(5): 517−522.

[23] CI L, RYU Z, JIN-PHILLIPP N Y, RÜHLE M. Investigation of the interfacial reaction between multi-walled carbon nanotubes and aluminum [J]. Acta Materialia, 2006, 54(20): 5367−5375.

[24] WANG X Q, MUJUMDAR A S. Heat transfer characteristics of nanofluids: A review [J]. International Journal of Thermal Sciences, 2007, 46(1): 1−19.

[25] PHILIP J, SHIMA P D. Thermal properties of nanofluids [J]. Adv Colloid Interface Sci, 2012, 183−184(15): 30−45.

[26] GÓMEZ S V, PIRIZ A F, DURÁN C J, PASTOR V J. Formation of oxygen structures by air activation: A study by FT-IR spectroscopy [J]. Carbon, 1999, 37(10): 1517−1528.

[27] MORENO C C, LOPEZ R M, CARRASCO M F. Changes in surface chemistry of activated carbons by wet oxidation [J]. Carbon, 2000, 38(14): 1995−2001.

[28] CAO G, CHOI H, OPORTUS J, KONISHI H, LI X. Study on tensile properties and microstructure of cast AZ91D/AlN nanocomposites [J]. Materials Science and Engineering: A, 2008, 494(1−2): 127−131.

[29] JIANG Q, LI X, WANG H. Fabrication of TiC particulate reinforced magnesium matrix composites [J]. Scripta Materialia, 2003, 48(6): 713−7.

[30] ZHAO Zhu-de, CHEN Qiang, WANG Yan-bin, SHU Da-yu. Microstructures and mechanical properties of AZ91D alloys with Y addition [J]. Materials Science and Engineering A, 2009, 515(1−2): 152−161.

[31] GOH C, WEI J, LEE L, GUPTA M. Ductility improvement and fatigue studies in Mg-CNT nanocomposites [J]. Composites Science and Technology, 2008, 68(6): 1432−1439.

[32] LI Q, VIERECKL A, ROTTMAIR CA, SINGER RF. Improved processing of carbon nanotube/magnesium alloy composites [J]. Composites Science and Technology, 2009, 69(7−8): 1193−1199.

[33] WANG S, CHOU C. Effect of adding Sc and Zr on grain refinement and ductility of AZ31 magnesium alloy [J]. Journal of Materials Processing Technology, 2008, 197(1−3): 116−121.

[34] BUSSIBA A, ARTZY A B, SHTECHMAN A, IFERGAN S, KUPIEC M. Grain refinement of AZ31 and ZK60 Mg alloys-towards superplasticity studies [J]. Materials Science and Engineering A, 2001, 302(1): 56−62.

[35] CZERWINSKI F. The generation of Mg−Al−Zn alloys by semisolid state mixing of particulate precursors [J]. Acta Materialia, 2004, 52(17): 5057−5069.

[36] ZHU T, CHEN Z W, GAO W. Effect of cooling conditions during casting on fraction of β-$Mg_{17}Al_{12}$ in Mg−9Al−1Zn cast alloy [J]. Journal of Alloys and Compounds, 2010, 501(2): 291−296.

[37] TATTERSALL H G, TAPPIN G. The work of fracture and its measurement in metals, ceramics and other materials [J]. Journal of Materials Science, 1966, 1(3): 296−301.

高性能碳纳米管增强 AZ91D 镁基复合材料的制备

袁秋红[1,2]，付东明[1]，曾效舒[1]，刘 勇[1]

1. 南昌大学 材料加工工程系，南昌 330031；
2. 新余学院 新能源科学与工程学院，新余 338000

摘 要：采用球磨加搅拌铸造工艺制备了 CNTs(质量分数为 0.1%)增强的 AZ91D 镁基复合材料。通过光学显微镜、X 射线衍射仪、傅里叶红外光谱仪、扫描电子显微镜、透射电子显微镜和室温拉伸试验对复合材料进行表征和分析。结果表明：碳纳米管在镁基体中分散很均匀，并且复合在基体中的碳纳米管结构较完整。与 AZ91D 基体相比，复合材料屈服强度和伸长率分别提高了 47.2%和 112.2%。碳纳米管在基体中的均匀分散且与基体形成的强界面结合使复合材料屈服强度和伸长率同时得到了提升。此外，晶粒细化和基体中均匀分散的 β 相($Mg_{17}Al_{12}$)也有助于复合材料力学性能的提高。

关键词：镁合金；碳纳米管；复合材料；铸造工艺；力学性能

(Edited by Yun-bin HE)